Environmental drivers of megafauna and hominin extinction in Southeast Asia

https://doi.org/10.1038/s41586-020-2810-y

Received: 25 March 2020

Accepted: 14 July 2020

Published online: 7 October 2020

Check for updates

Julien Louys[1,2]✉ & Patrick Roberts[3,4,5]✉

Southeast Asia has emerged as an important region for understanding hominin and mammalian migrations and extinctions. High-profile discoveries have shown that Southeast Asia has been home to at least five members of the genus *Homo*[1–3]. Considerable turnover in Pleistocene megafauna has previously been linked with these hominins or with climate change[4], although the region is often left out of discussions of megafauna extinctions. In the traditional hominin evolutionary core of Africa, attempts to establish the environmental context of hominin evolution and its association with faunal changes have long been informed by stable isotope methodologies[5,6]. However, such studies have largely been neglected in Southeast Asia. Here we present a large-scale dataset of stable isotope data for Southeast Asian mammals that spans the Quaternary period. Our results demonstrate that the forests of the Early Pleistocene had given way to savannahs by the Middle Pleistocene, which led to the spread of grazers and extinction of browsers—although geochronological limitations mean that not all samples can be resolved to glacial or interglacial periods. Savannahs retreated by the Late Pleistocene and had completely disappeared by the Holocene epoch, when they were replaced by highly stratified closed-canopy rainforest. This resulted in the ascendency of rainforest-adapted species as well as *Homo sapiens*—which has a unique adaptive plasticity among hominins—at the expense of savannah and woodland specialists, including *Homo erectus*. At present, megafauna are restricted to rainforests and are severely threatened by anthropogenic deforestation.

Southeast Asia—comprising the northern Indochinese and southern Sundaic subregions (Fig. 1)—is characterized by extensive dipterocarp rainforests, which host some of the most species-rich ecosystems on Earth. Yet, the exposure of a now-submerged Sundaland continental shelf during periods of lower sea level is argued to have catalysed severe environmental change in the region—most notably, the development of a central savannah corridor that stretched from the biogeographical region of Indochina to the island of Java[7,8]. Supported by changes in the intertropical convergence zone that substantially reduced precipitation over much of Southeast Asia, the expansion of drier, grassland environments has been argued to have channelled early species of *Homo* and large grazing taxa throughout much of mainland and island Southeast Asia[9–11]. The later disappearance of the corridor and expansion of the modern rainforest has been proposed to have led to the extinction or range reduction of many of these former travellers[4]. Meanwhile, these changes are also associated with population expansions of rainforest species, such as the Bornean orangutan and the Asian golden cat[12,13]. Given the emerging view of Pleistocene Southeast Asia as a cosmopolitan region, testing these hypotheses will make a major contribution to global understandings of how hominin taxa had different ecological tolerances or capacities[14], and of the role of climate change in driving megafauna extinctions[15].

Despite evidence that suggests more-open environments were present in the Pleistocene[7,8,16], the extent—and even existence—of the Southeast Asian savannah corridor remains hotly debated, as some modelling and long-distance pollen data suggest there was rainforest coverage even at the peak of the Last Glacial Maximum[14,15,17–19]. Testing these propositions has been hindered by limited palaeo-environmental data associated with local records and a lack of a widespread palaeo-ecological assessment. Stable carbon ($\delta^{13}C$) and oxygen ($\delta^{18}O$) isotope analyses have long been used to reconstruct major environmental events on local, continental and global scales. Built on the principles that plants have distinct $\delta^{13}C$ values depending on their photosynthetic pathway and that $\delta^{18}O$ values vary with environmental water, research has focused on the degree to which the medium- and large-bodied mammals associated with hominin archaeological and palaeontological sites provide evidence for more-humid forest and woodland ecologies dominated by C_3 plants versus open, drier 'savannah' biomes characterized by C_4 plants[20]. The application of isotope analyses in Southeast Asia has historically been relatively limited, although recent studies have begun analysing fossil mammals as palaeo-environmental indicators (Extended Data Table 1). Importantly, the modern baseline data that are necessary to properly interpret the fossil record and to put

[1]Australian Research Centre for Human Evolution, Environmental Futures Research Institute, Griffith University, Brisbane, Queensland, Australia. [2]College of Asia and the Pacific, The Australian National University, Canberra, Australia Capital Territory, Australia. [3]Max Planck Institute for the Science of Human History, Jena, Germany. [4]School of Social Science, The University of Queensland, Brisbane, Queensland, Australia. [5]Archaeological Studies Programme, University of the Philippines, Quezon City, The Philippines. ✉e-mail: j.louys@griffith.edu.au; roberts@shh.mpg.de

Fig. 1 | Map of the Indochinese and Sundaic subregions. Locality map showing the biogeographical subregions examined, land extent during the Last Glacial Maximum and the proposed extent of the 'savannah' corridor (after ref. [7]). Map from CartoGIS CAP Australian National University 20-217_KP.

the deep-time record of geobiology into a modern context have been almost entirely missing.

To address this deficit, we report $\delta^{13}C$ and $\delta^{18}O$ data for 269 modern and historical specimens, representing 63 species of mammal found in Southeast Asia. We compare these to 644 previously published $\delta^{13}C$ and $\delta^{18}O$ values from fossil taxa that span from the Early Pleistocene to the present. For consistency and comparability, in all cases the $\delta^{13}C$ values obtained from the specimens have been corrected to an estimate of the $\delta^{13}C$ value of the diet of the mammal ($\delta^{13}C_{diet}$). To our knowledge, our combined dataset represents the largest compilation of $\delta^{13}C$ and $\delta^{18}O$ data from mammals in Asia, and allows us to examine broad trends in the distribution of C_3 and C_4 plants associated with faunal communities and hominins over time.

Our results show that during the Early Pleistocene, consumers of both C_3 and C_4 resources were present in Southeast Asia (Fig. 2). However, these mammals were unevenly distributed across the region (Extended Data Table 2); consumers of C_3 resources were predominately found in Indochina ($\delta^{13}C_{diet}$ quartile 1 to quartile 3 range (Q1–Q3) of −29.3‰ to −26.4‰), and consumers of C_4 resources were located largely in Sundaland ($\delta^{13}C_{diet}$ Q1–Q3 of −20.0‰ to −13.3‰). The distribution of herbivores and omnivores was not significantly different across ecosystems dominated by C_3 or C_4 plants (Extended Data Fig. 1) during this period (χ^2 (2, n = 120) = 1.95, P = 0.377). By the Middle Pleistocene, Sundaland records very few consumers of C_3 resources (Extended Data Figs. 1, 2); most species fall into the range associated with feeding on C_4 resources or—to a lesser extent—mixed feeding on C_3 and C_4 resources (Q1–Q3 of −15.8‰ to −13.3‰). The beginning of the Middle Pleistocene sees a peak in $\delta^{13}C_{diet}$ (Extended Data Fig. 2), which—in Indochina—corresponds to a shift of herbivores consuming C_3 plants towards higher $\delta^{13}C$ values (χ^2 (2, n = 308) = 40.754, P < 0.001). This appears not to have affected omnivores, the distributions of which across both regions remain similar to their Early Pleistocene distributions (χ^2 (2, n = 39) = 0.23, P = 0.893). Carnivores favour grazers of C_4 plants during this time ($\bar{x}$ = −14.6‰, n = 7). By the Late Pleistocene, most Sundanese and Indochinese herbivores and omnivores were consuming predominately C_3 resources ($\bar{x}_{herbivore}$ = −25.3‰, n = 149 and $\bar{x}_{omnivore}$ = −22.3‰, n = 38). This stands in marked contrast to the carnivores, most of which were found at the C_4 end of the dietary spectrum ($\bar{x}_{carnivore}$ = −16.2‰, n = 14). By the Holocene, Southeast Asian mammals were consuming diets dominated by C_3 resources across the entire trophic spectrum ($\bar{x}_{herbivore}$ = −25.5‰, n = 270; $\bar{x}_{omnivore}$ = −23.5‰, n = 38; and $\bar{x}_{carnivore}$ = −24.0‰, n = 15).

Beyond prominent distinctions between C_3 and C_4 resources, we also find considerable variation in $\delta^{13}C$ and $\delta^{18}O$ values within ecosystems dominated by C_3 plants. The lowest $\delta^{13}C_{diet}$ values (below −29.0‰) correspond to closed-canopy and subcanopy habitats[21,22]. Conversely,

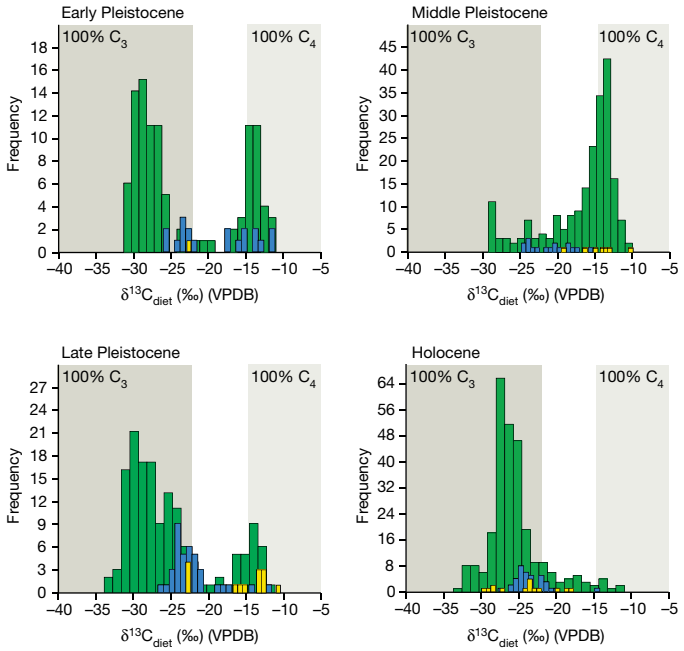

Fig. 2 | Distribution of $\delta^{13}C$ values across geological subepochs and epochs. Green bars, herbivores; blue bars, omnivores; yellow bars, carnivores. Shaded boxes represent the division between forests (consumers of 100% C_3 resources) and grasslands (consumers of 100% C_4 resources). All large-herbivore $\delta^{13}C$ values from enamel ($\delta^{13}C_{enamel}$) were adjusted by −14‰; omnivores, rodents, pigs and primates were adjusted by −11‰; Carnivora by −9‰; $\delta^{13}C$ values from hair or horn ($\delta^{13}C_{hair/horn}$) were adjusted by −3.1‰; samples from after AD 1930 were adjusted by 1.5‰. VPDB, Vienna PeeDee Belemnite.

higher $\delta^{13}C$ values (−25.6 to −23.0‰) occur in open-canopy forests or woodlands. High $\delta^{18}O$ values are also found in folivores that forage in the upper canopy, whereas folivores that prefer the understorey have lower $\delta^{18}O$ values[23]. In Southeast Asia, the distribution of $\delta^{13}C$ and $\delta^{18}O$ values in browsers are significantly different across all subepochs (Kruskal–Wallis test, $H_C = 25.23$, $P < 0.001$; $H_o = 27.34$, $P < 0.001$). Post hoc analysis indicates that significant differences in environmental structure are present through time (Extended Data Fig. 3). In the Early Pleistocene, sites in Indochina have some browsers that, based on their $\delta^{13}C$ values, were feeding on the understorey. By the Middle Pleistocene, no understory browsers are recorded and only five individuals have values consistent with closed canopies. In the Late Pleistocene, sites in northern Indochina begin to record the first clear evidence of stratified closed-canopy forests. In the Holocene, browsers in both Indochina and Sundaland occupy closed-canopy forests, with both regions exhibiting highly negatively skewed distributions (−0.53 and −0.63, respectively). Increased forest stratification through time is suggested by the emergence of canopy specialists in the Holocene, which is supported by progressively, significantly higher $\delta^{18}O$ values among species that forage in the lower, middle and upper canopies (Kruskal–Wallis test, $H = 13.95$, $P = 0.001$).

The regional shifts in the consumption of C_3 and C_4 resources across all taxa, and the shifts in $\delta^{13}C$ and $\delta^{18}O$ values within browsing groups, reveal a common picture. Although subtle variation in atmospheric CO_2 partial pressure and $\delta^{13}C$ values may have occurred over time (which will affect interpretations of $\delta^{13}C$ values as being exactly equivalent to forest cover), these are not enough to obfuscate the magnitude of changes observed in terms of the relative abundance of C_4 and C_3 resources or environmental shifts within C_3-resource-dominated environments[20]. Our data show that mixed to closed-canopy forests were present in Indochina during the Early Pleistocene, at which time Sundaland hosted open savannah grasslands. By the beginning of the Middle Pleistocene, both regions were dominated by open savannahs—although the savannahs of Indochina were more wooded than those of Sundaland, and some open forests persisted. Closed-canopy forests emerged in Indochina during the Late Pleistocene, while Sundaland remained largely dominated by open-canopy forests. By the Holocene, both regions were dominated by closed-canopy forests.

These observed shifts are consistent with global climate models for the Quaternary, which indicate a substantial change at the mid-Pleistocene transition. A shift from low-amplitude 41,000-year cycles to high-amplitude 100,000-year cycles between 1.25 million years ago (Ma) and 700 thousand years ago (ka) was accompanied by considerable decreases in sea surface temperatures, increases in ice volume, and heightened Asian aridity and monsoonal intensity[24]. The change in glacial cycles, recorded in the benthic oxygen isotope record, coincides with our observed peak in $\delta^{13}C$ and $\delta^{18}O$ values in Southeast Asian mammals (Extended Data Fig. 2). As drier conditions decreased in intensity, savannahs began to give way to forests (Methods). This process was further affected at 400 ka by the subsidence of the Sunda shelf[25]. This event markedly reduced exposed land and decreased albedo, which led to increased atmospheric convection and regional rainfall[26]. Our data show an accelerated decrease in $\delta^{13}C$ and $\delta^{18}O$ values at this time (Extended Data Fig. 2a, b), indicating a continued trend towards conditions that were more favourable for forests.

The distribution of sites suggests that—at their maximum—savannahs extended from Indochina down into Sundaland, enabling the dispersal of large-bodied grazers across this vast region. The expansion of these ecosystems coincides with the time of maximum hominin diversity in the region[2]. During the Middle Pleistocene and beginning of the Late Pleistocene, the notable decline of habitats dominated by C_4 resources occurs at a time at which almost all hominin taxa present in Southeast Asia disappear. These hominin populations were seemingly unable to flexibly shift to the expanding tropical rainforest habitats that came to dominate in Southeast Asia (Table 1), which highlights the likely status of these species as reliant on mixed savannah and woodland environments[10]. By contrast, the arrival of *Homo sapiens* in the region at about 72–45 ka occurs at a time of expanded presence of tropical lowland evergreen rainforest. Although savannah settings may have persisted in some patches and were almost certainly used by our species, *H. sapiens* expanded its niche in Southeast Asia to make use of rich rainforest and marine habitats[27,28]. The ability to specialize in such environments becomes increasingly evident in the Terminal Pleistocene and Holocene[29].

Beyond hominins, these environmental shifts had a major role in mammalian turnover more broadly. During the Early Pleistocene, most mammals occupied a broad ecospace of open forests: the only exception was perissodactyls, which were restricted to closed-canopy forests (Extended Data Fig. 4). The expansion of environments dominated by C_4 resources and the decline of closed-canopy forest biomes between the Early and Middle Pleistocene saw mammals occupy one of two ecospaces: open forests or savannahs. Rodents, primates and perissodactyls retreated to open forests, whereas carnivores, artiodactyls and proboscideans took advantage of the savannahs. The loss of forests probably had a role in the extinction of the largest ape ever to have existed, *Gigantopithecus blacki* (Table 1). On the basis of stable isotope data, associated fauna and tooth morphology, this species appears to have been specialized in rainforest conditions in northern Indochina, and its extinction during the Middle Pleistocene was probably driven by loss of its preferred habitats[4]. These changes probably also contributed to the extinction of other Early Pleistocene browsers, such as *Ailuropoda wulingshanensis* and *Sus peii* (Table 1). The large-scale distribution of savannahs during the Middle Pleistocene—when most of the region that is now islands was directly connected to the mainland—produced novel faunal communities across Sundaland, such as the faunas from the sites of Trinil H. K., Kedung Brubus and Ngandong, through exchange with Indochina and local endemism[11].

Table 1 | Extinct megafauna, dates of their last appearance and isotope values

Taxon (common name)	Date of last appearance	MIS	Mean $\delta^{13}C$	Mean $\delta^{18}O$
Ailuropoda baconi (Bacon's giant panda)	12–10 ka (Gulin)	MIS 1	−25.6 (4)	−7.0 (4)
Ailuropoda wulingshanensis (Wulingshan panda)	1.2 Ma (Sanhe)	MIS 35–40	−25.7 (1)	−7.7 (1)
Axis lydekkeri (Lydekker's deer)	117–108 ka (Ngandong)	MIS 5	−13.8 (7)	−4.2 (7)
Bubalus palaeokerabau	117–108 ka (Ngandong)	MIS 5	−14.6 (19)	−4.7 (19)
Crocuta crocuta ultima (Spotted hyena)	25–18 ka (Boh Dambang)	MIS 2	−14.8 (12)	−6.3 (4)
Duboisia santeng (Dubois' antelope)	0.54–0.43 Ma (Trinil)	MIS 12–14	−14.0 (3)	−4.1 (3)
Elephas hysudrindicus	117–108 ka (Ngandong)	MIS 5	−15.0 (12)	−4.6 (12)
Gigantopithecus blacki	400–320 ka (Hejiang Cave)	MIS 9–11	−26.6 (17)	−6.4 (17)
Homo erectus	117–108 ka (Ngandong)	MIS 5	−16.5 (7)	−6.3 (7)
Megatapirus augustus (giant tapir)	12–10 ka (Gulin)	MIS 1	−30.2 (3)	−6.5 (3)
Pachycrocuta brevirostris (short-faced hyena)	196 and 143 ka (Changyang)	MIS 6	−22.7 (1)	−9.8 (1)
Sinomastodon bumiajuensis	1.9–1.2 Ma (Sangiran)	MIS 35–72	−16.5 (8)	−5.0 (8)
Stegodon orientalis	12–10 ka (Gulin)	MIS 1	−25.5 (20)	−6.8 (20)
Stegodon trigonocephalus	117–108 ka (Ngandong)	MIS 5	−14.4 (55)	−6.1 (55)
Stegoloxodon indonesicus	>1.5 Ma (Kaliglagah Formation)	>MIS 50	−27.7 (5)	−5.7 (5)
Sus brachygnathus	0.54–0.43 Ma (Trinil)	MIS 12–14	−17.8 (3)	−6.3 (3)
Sus peii	810–630 ka (Sanhe Cave)	MIS 15–20	−25.8 (1)	−7.5 (1)
Sus xiaozhu	400–320 ka (Hejiang Cave)	MIS 9–11	−23.5 (1)	−7.8 (1)
Tapirus sinensis (Chinese tapir)	<280–88 ka (Lower Pubu Cave)	<MIS 5	−29.5 (4)	−10.7 (4)

Sites at which the taxon was found are listed in parentheses after the date of last appearance, and approximate Marine Isotope Stage(s) (MIS) for these sites are given. Mean $\delta^{13}C$ and $\delta^{18}O$ values are provided (with the number of individual specimens in parentheses): $\delta^{13}C < 21‰$ is considered typical of ecosystems dominated by C_3 resources[22].

In turn, a return shift towards denser tropical canopies from the late Middle Pleistocene onwards seemingly contributed to extinctions of grazing specialists that had, by this time, become widely dispersed. Artiodactyls shift towards open-canopy forest environments (Extended Data Fig. 4), and this period records the last appearance of grazers such as *Bubalus palaeokerabau* and *Duboisia santeng*; this ecospace also hosts primates and rodents, as it predominantly did in the Middle Pleistocene. However, this change pales in comparison to the enormous shift in diet exhibited by proboscideans, which corresponds to the loss of grazing taxa including *Elephas hysudrindicus* and *Stegodon trigonocephalus* (Table 1). From this point onwards, elephants and their kin became restricted to closed-canopy forests. Rhinoceroses and tapirs return to closed-canopy forests by the Late Pleistocene, although they were affected by an apparent reduction in rainforests during the Last Glacial Maximum; for example, Sumatran rhinos show a population decline that corresponds to this period[30]. The Late Pleistocene saw a marked move towards forest ecosystems for carnivores and a major extinction event for hyenas, which were adapted to open environments. Finally, the Holocene witnessed the expansion of major forested ecospaces: open- and closed-canopy forests. Primates also demonstrate a shift towards forests with a more-closed canopy at this time.

There is a significant positive correlation between conservation status and extinction status in Southeast Asian mammals for both $\delta^{13}C$ and $\delta^{18}O$ values ($\tau_c = 0.14$, $P < 0.001$; $\tau_o = 0.16$, $P < 0.001$), which indicates that the loss of drier and more-open environments is associated with a higher risk of extinction. The correlation remains significant even if only modern species are considered; however, the trend is reversed, such that rainforest-adapted taxa are correlated with higher levels of extinction risk ($\tau_c = -0.18$, $P < 0.001$; $\tau_o = 0.09$, $P = 0.006$). Thus, our data shows that megafauna extinctions in the Early to Middle Pleistocene predominantly involved taxa adapted to C_4 resources, as these taxa faced the re-expansion of Late Pleistocene forest and the loss of the savannahs that had previously sustained them. By contrast, rainforest species are currently at the greatest risk of extinction. This highlights the dominant role of environmental change in the fortunes of large-bodied mammals. The modern rainforests of Southeast Asia contain some of the most critically endangered animals in the world. They are at risk from overhunting and loss of habitat through deforestation[31], which represents an anthropogenically influenced return to the grassland ecosystems in which these rainforest taxa were notably absent. Our long-term perspective thus provides critical insights that are relevant to current conservation priorities. For example, orangutan (*Pongo* spp.) diets differ significantly across all subepochs (Kruskal–Wallis test, $H = 11.11$, $P = 0.011$), with the lowest mean $\delta^{13}C$ values being found during the Holocene. These changes are probably tied to increased exploitation and land clearing by people during the mid-to-late Holocene, which drove orangutans deeper into rainforests where they are isolated and vulnerable[32].

Robust palaeo-ecological datasets are essential if we are to understand the changing adaptations of hominins and other megafauna during the Quaternary. Although such records have long been available from Africa, they have been absent from Southeast Asia until recently. Our results demonstrate that the coming and going of extensive savannah environments had a major role in hominin and mammalian Pleistocene biogeography, with savannah- and woodland-adapted fauna being usurped by rainforest-adapted species as the former habitats increasingly disappeared during the late Middle Pleistocene and Late Pleistocene. Of the once-high hominin diversity in the region, it was only our species that sufficiently adapted to the changing conditions. At present, a return to more-open grassland conditions—with human development, plantations and population growth as its primary driver—stands as the greatest threat to some of the most critically endangered mammals in the world, as well as the long-term sustainability of human populations in the region and across the tropics as a whole. Our work helps to place these threats in their long-term context, demonstrating that, while the fortunes of our own species changed for the better with the arrival of the typical endemic rainforest communities, we are now in danger of destroying these ecosystems forever.

Online content

Any methods, additional references, Nature Research reporting summaries, source data, extended data, supplementary information, acknowledgements, peer review information; details of author contributions and competing interests; and statements of data and code availability are available at https://doi.org/10.1038/s41586-020-2810-y.

1. Détroit, F. et al. A new species of *Homo* from the Late Pleistocene of the Philippines. *Nature* **568**, 181–186 (2019).

2. Kaifu, Y. Archaic hominin populations in Asia before the arrival of modern humans: their phylogeny and implications for the "Southern Denisovans". *Curr. Anthropol*. **58**, S418–S433 (2017).
3. Reich, D. et al. Denisova admixture and the first modern human dispersals into Southeast Asia and Oceania. *Am. J. Hum. Genet*. **89**, 516–528 (2011).
4. Louys, J., Curnoe, D. & Tong, H. Characteristics of Pleistocene megafauna extinctions in Southeast Asia. *Palaeogeogr. Palaeoclimatol. Palaeoecol*. **243**, 152–173 (2007).
5. Klein, R. G. Stable carbon isotopes and human evolution. *Proc. Natl Acad. Sci. USA* **110**, 10470–10472 (2013).
6. Cerling, T. E. et al. Woody cover and hominin environments in the past 6 million years. *Nature* **476**, 51–56 (2011).
7. Heaney, L. R. in *Tropical Forests and Climate* (ed. Myers, N.) 53–61 (Springer, 1991).
8. Bird, M. I., Taylor, D. & Hunt, C. Palaeoenvironments of insular Southeast Asia during the Last Glacial Period: a savanna corridor in Sundaland? *Quat. Sci. Rev*. **24**, 2228–2242 (2005).
9. Louys, J. & Turner, A. Environment, preferred habitats and potential refugia for Pleistocene *Homo* in Southeast Asia. *C. R. Palevol* **11**, 203–211 (2012).
10. Dennell, R. & Roebroeks, W. An Asian perspective on early human dispersal from Africa. *Nature* **438**, 1099–1104 (2005).
11. van den Bergh, G. D., de Vos, J. & Sondaar, P. Y. The Late Quaternary palaeogeography of mammal evolution in the Indonesian Archipelago. *Palaeogeogr. Palaeoclimatol. Palaeoecol*. **171**, 385–408 (2001).
12. Steiper, M. E. Population history, biogeography, and taxonomy of orangutans (Genus: *Pongo*) based on a population genetic meta-analysis of multiple loci. *J. Hum. Evol*. **50**, 509–522 (2006).
13. Patel, R. P. et al. Two species of Southeast Asian cats in the genus *Catopuma* with diverging histories: an island endemic forest specialist and a widespread habitat generalist. *R. Soc. Open Sci*. **3**, 160350 (2016).
14. Cannon, C. H., Morley, R. J. & Bush, A. B. G. The current refugial rainforests of Sundaland are unrepresentative of their biogeographic past and highly vulnerable to disturbance. *Proc. Natl Acad. Sci. USA* **106**, 11188–11193 (2009).
15. Sun, X., Li, X., Luo, Y. & Chen, X. The vegetation and climate at the last glaciation on the emerged continental shelf of the South China Sea. *Palaeogeogr. Palaeoclimatol. Palaeoecol*. **160**, 301–316 (2000).
16. Louys, J. & Meijaard, E. Palaeoecology of Southeast Asian megafauna-bearing sites from the Pleistocene and a review of environmental changes in the region. *J. Biogeogr*. **37**, 1432–1449 (2010).
17. Raes, N. et al. Historical distribution of Sundaland's dipterocarp rainforests at Quaternary glacial maxima. *Proc. Natl Acad. Sci. USA* **111**, 16790–16795 (2014).
18. Handiani, D. et al. Tropical vegetation response to Heinrich Event 1 as simulated with the UVic ESCM and CCSM3. *Clim. Past Discuss*. **8**, 5359–5387 (2012).
19. Chabangborn, A., Brandefelt, J. & Wohlfarth, B. Asian monsoon climate during the Last Glacial Maximum: palaeo-data–model comparisons: LGM Asian monsoon climate. *Boreas* **43**, 220–242 (2014).
20. Levin, N. E. et al. Herbivore enamel carbon isotopic composition and the environmental context of *Ardipithecus* at Gona, *Ethiopia. Geol. S. Am. S*. **446**, 215–235 (2008).
21. Cerling, T. E., Hart, J. A. & Hart, T. B. Stable isotope ecology in the Ituri Forest. *Oecologia* **138**, 5–12 (2004).
22. Secord, R., Wing, S. L. & Chew, A. Stable isotopes in early Eocene mammals as indicators of forest canopy structure and resource partitioning. *Paleobiology* **34**, 282–300 (2008).
23. Fannin, L. D. & McGraw, W. S. Does oxygen stable isotope composition in primates vary as a function of vertical stratification or folivorous behaviour? *Folia Primatol*. **91**, 219–227 (2020).
24. Clark, P. U. et al. The middle Pleistocene transition: characteristics, mechanisms, and implications for long-term changes in atmospheric pCO_2. *Quat. Sci. Rev*. **25**, 3150–3184 (2006).
25. Sarr, A. C. et al. Subsiding Sundaland. *Geology* **47**, 119–122 (2019).
26. Di Nezio, P. N. et al. The climate response of the Indo-Pacific warm pool to glacial sea level. *Paleoceanogr* **31**, 866–894 (2016).
27. Roberts, P. et al. Isotopic evidence for initial coastal colonization and subsequent diversification in the human occupation of Wallacea. *Nat. Commun*. **11**, 2068 (2020).
28. Barker, G. & Farr, L. E. *Archaeological Investigations in the Niah Caves, Sarawak, The Archaeology of Niah Caves, Sarawak* (McDonald Institute Monographs, 2016).
29. Piper, P. J. & Rabett, R. J. Hunting in a tropical rainforest: evidence from the Terminal Pleistocene at Lobang Hangus, Niah Caves, Sarawak. *Int. J. Osteoarchaeol*. **19**, 551–565 (2009).
30. Steiner, C. C., Houck, M. L. & Ryder, O. A. Genetic variation of complete mitochondrial genome sequences of the Sumatran rhinoceros (*Dicerorhinus sumatrensis*). *Conserv. Genet*. **19**, 397–408 (2018).
31. Sodhi, N. S., Koh, L. P., Brook, B. W. & Ng, P. K. Southeast Asian biodiversity: an impending disaster. *Trends Ecol. Evol*. **19**, 654–660 (2004).
32. Spehar, S. N. et al. Orangutans venture out of the rainforest and into the Anthropocene. *Sci. Adv*. **4**, e1701422 (2018).

Publisher's note Springer Nature remains neutral with regard to jurisdictional claims in published maps and institutional affiliations.

© The Author(s), under exclusive licence to Springer Nature Limited 2020

Methods

No statistical methods were used to predetermine sample size. The experiments were not randomized and investigators were not blinded to allocation during experiments and outcome assessment.

The process of photosynthesis produces strong isotopic fractionation of ^{13}C, depending on the photosynthetic pathway used by the plant[33,34]. There is a large and nonoverlapping distinction between C_3 and C_4 plants[35]. On average, depletion is −5‰ in C_4 and −19‰ in C_3 plants, relative to atmospheric $\delta^{13}CO_2$ (approximately −6.5‰ before AD 1930). This distinction has been used in the tropics and subtropics to determine the relative proportion of grassland (dominated by C_4 plants) to woodland or forest (dominated by C_3 plants) in mammalian (including hominin) diets, and thus to infer the associated environments[33–39]. Under C_3-dominated forest settings, there is a further canopy influence on the isotopic composition of plants. Lower light levels and the trapping of respired CO_2 leads to an even stronger depletion in ^{13}C in soils, leaves and fruits—and therefore mammals—found in subcanopy environments[21,40,41]. This 'canopy effect' has been observed in temperate, subtropical and tropical forests[41–46]. The distribution of $\delta^{13}C$ values in tropical-forest mammal communities has a long left tail (highly negative skew), reflecting the abundance of browsers feeding in the canopy top, gaps in the canopy and subcanopy frugivores, which have higher $\delta^{13}C$ values than browsers that feed only in the subcanopy[21,22].

Measurements of $\delta^{18}O$ values in vegetation and animals can also provide important insights into palaeo-environments and the presence of closed-canopy forests. The critical site of isotope fractionation in vegetation is the leaf, with evaporation leading to a loss of lighter ^{16}O and concomitant enrichment in ^{18}O (ref. [47]). The degree of $\delta^{18}O$ enrichment in leaf water is thus negatively related to relative humidity, with increasing humidity resulting in decreased $\delta^{18}O$ values and vice versa[48–50]. Owing to differences in evaporative potentials across different strata in the canopy and between different plant parts found at different heights, CO_2 and vegetation $\delta^{18}O$ will differ on the basis of vertical stratification[51–53]. In tropical systems, the $\delta^{18}O$ values of vegetation, recorded with particularly high fidelity in the tissues of mammals that obtain most of their water requirements from plants, provide information on evaporative potential or the source effect of rainfall as well as the vertical structure of forests[23,51,52,54–57]. Notably, folivores that forage in the canopy top will have higher $\delta^{18}O$ values than those animals that prefer the subcanopy[23].

Historical mammal specimens were selected for $\delta^{13}C$ and $\delta^{18}O$ analysis of tooth enamel from the collections of the Zoologische Staatssammlung München, the Muséum National d'Histoire Naturelle, the American Museum of Natural History and the Lee Kong Chian Natural History Museum. Specimens with full adult dentition in occlusion and with clear provenance and collection information were preferentially selected. In collaboration with the curatorial teams of each institution, specimens were sampled only where duplicate specimens existed for the same taxa. Sampling was done under the CITES (Convention on International Trade in Endangered Species of Wild Fauna and Flora) registration of Griffith University (no. AU 062) and the Department of Archaeology, Max Planck Institute for the Science of Human History (no. DE 215-07). Specimens were identified on the basis of existing labels within the museum collections, and taxonomy was updated according to the latest available systematic information.

Sampled teeth were cleaned using portable air abrasion to remove any adhering external material. Enamel powder for bulk analysis was obtained using gentle abrasion with a diamond-tipped drill along the full length of the buccal surface to ensure a representative measurement for the entire period of enamel formation. All enamel powder was pretreated to remove organic or secondary carbonate contaminates, following established protocols. This consisted of a series of washes in 1.5% sodium hypochlorite for 60 min, followed by 3 rinses in purified H_2O and centrifuging, before 0.1 M acetic acid was added for 10 min, followed by another 3 rinses in purified H_2O (as per refs. [58,59]). When comparing the newly acquired data presented here with those from the existing literature, it is worth noting that different pretreatment protocols have been applied in each case—although, for tooth enamel, pretreatment-induced variation is limited (<0.5‰ for $\delta^{13}C$ and $\delta^{18}O$)[60,61] and these differences have a negligible effect at the scale of the questions examined here[62].

Following reaction with 100% phosphoric acid, gases evolved from the samples were analysed for their stable carbon and oxygen isotopic measurements using a Thermo Gas Bench 2 connected to a Thermo Delta V Advantage Mass Spectrometer at the Department of Archaeology, Max Planck Institute for the Science of Human History. $\delta^{13}C$ and $\delta^{18}O$ values were compared against International Standards (IAEA-603 ($\delta^{13}C = 2.5$; $\delta^{18}O = -2.4$); IAEA-CO-8 ($\delta^{13}C = -5.8$; $\delta^{18}O = -22.7$); USGS44 ($\delta^{13}C = -42.2$)) and an in-house standard (MERCK ($\delta^{13}C = -41.3$; $\delta^{18}O = -14.4$)). Replicate analysis of MERCK standards suggests that machine measurement error is about ±0.1‰ for $\delta^{13}C$ values and ±0.2‰ for $\delta^{18}O$ values. Overall measurement precision was studied through the measurement of repeat extracts from a bovid tooth enamel standard ($n = 30$, ±0.2‰ for both $\delta^{13}C$ and $\delta^{18}O$ values).

Fossil $\delta^{13}C$ and $\delta^{18}O$ values were compiled from existing published sources[63–75]. These cover 31 sites across Indochina and Sundaland, representing—to our knowledge—the largest compilation of stable isotope data from anywhere in Asia. $\delta^{13}C$ and $\delta^{18}O$ analysis of fossil tooth enamel has previously been shown to preserve ecological distinctions back into the Miocene epoch[37,76]. The bioapatite of tooth enamel has fewer substitutions, less distortion and larger crystals than that found in bone and dentine, which makes it more resistant to taphonomic alteration[77,78]. Although we have not been able to check the state of each tooth sampled in the studies we have compiled, a number of studies have studied the potential for taphonomic change in fossil enamel in hydrologically active tropical settings using chemical and physical analysis[27,59]. They found limited alteration to fossil enamel structure in both open-air and cave contexts in South and Southeast Asia dating back to the Pleistocene, and concluded there was no reason to assume alteration to the $\delta^{13}C$ and $\delta^{18}O$ values. Furthermore, several studies from which the compiled data were taken applied similar approaches to demonstrate taphonomic integrity[64,72,75].

Where serially sampled values were provided, we calculated the mean for both carbon and oxygen isotopes for each specimen. To enable comparison of our $\delta^{13}C$ dataset with existing fossil enamel $\delta^{13}C$ values in the literature we performed a series of data corrections. We made no adjustment for the Suess effect for specimens collected before 1931, as $\delta^{13}C$ CO_2 in 1930 differs from pre-industrial values only by around 0.2‰[79]. As far as can be confidently ascertained from existing museum records, this is after or around the time of the death of most individual animals sampled in our dataset. For specimens with known collection dates after 1930, we applied an offset of 1.5‰ and for modern data sourced from published sources we followed the authors' application of this offset. Another approach is to correct modern samples using the atmospheric $\delta^{13}C$ values by year, using a dataset that spans 1850–2015[80]. The use of different corrections produced statistically indistinguishable values ($r = 0.99$, $P < 0.0001$), lending confidence to the modern $\delta^{13}C$ values used in our analyses. To convert all existing faunal data into an estimated $\delta^{13}C$ of diet, a correction was applied to all fossil and modern enamel, apatite, bone, horn and hair samples.

Hair and horn samples were adjusted by −3.1‰, following refs. [63,81,82]. Enamel, apatite and bone samples from both ruminant and nonruminant large-bodied herbivores were adjusted by −14‰. This corresponds to a collagen-to-diet offset of about −5‰ (following ref. [75]) and a carbonate-to-collagen offset of between −7 and −8‰, and −9‰, for nonruminants and ruminants, respectively[82,83]. Because they have similar carbonate-to-collagen offsets (wild omnivores (−5.5‰), omnivorous rodents (−5.5‰), captive pigs (−6.0‰), hominoids (−6.0‰) and cercopithecines (−5.9‰)[83]), we adjusted all omnivores, rodents, pigs

and primates in our dataset by −11‰. Several taxa in Asia belonging to the Carnivora are herbivores (for example, giant panda and red panda). Diet–apatite offset values are determined largely by digestive physiology, with differences in metabolic breakdown (and, in particular, the degree of fermentation) being a likely explanation for differences between carnivores and herbivores[84,85]. Fermentation processes are in turn controlled by gut microbiota[86]. We assigned offset values for herbivorous Carnivora on the basis of comparative gut microorganism diversity and physiology[87,88]. On this basis, giant and red pandas are similar to other typical carnivores (supplementary figure 2 in ref. [87]). Thus, all Carnivora were adjusted by −9‰, as the carnivore carbonate-to-collagen offset is lower than that observed in other mammals[84].

All statistical analyses were run in PAST v.2.17c[89]. Univariate statistics for each geological subepoch, and region and trophic group listed, are provided in Extended Data Tables 2, 3, respectively. To test whether the distributions of herbivores and omnivores were bimodal for the Early and Middle Pleistocene, we subjected each group (that is, Early Pleistocene herbivores, Early Pleistocene omnivores, Middle Pleistocene herbivores and Middle Pleistocene herbivores) to a *k*-means cluster analysis, setting the number of clusters to two. We then counted the number of values that fell into the first and second clusters, corresponding to C_3 and C_4 peaks, respectively. Division across all groups was very similar, with the division between clusters discernible in all but one case at −20.0‰ $\delta^{13}C$. The only exception was the Middle Pleistocene herbivores, for which the division occurred between −19.3‰ and 19.5‰. Full counts were used in the χ^2 test (Extended Data Table 4). For consistency, we use a cut-off at −20.0‰ across all groups; however, even when using the value of −19.4‰ for Middle Pleistocene herbivores, they are still significantly different to their Early Pleistocene counterparts (χ^2 (2, n = 208) = 48.195, P < 0.001).

Each epoch and subepoch of the Quaternary samples vastly different temporal scales and includes different numbers of glacial–interglacial cycles. Thus, grouping sites by geological group may mask or extenuate vegetation trends that are not reflective of the past 2.6 million years. To examine long-term trends in $\delta^{13}C$ and $\delta^{18}O$ values through the Quaternary, for sites with published age estimations (Extended Data Table 5), we calculated the average $\delta^{13}C$ and $\delta^{18}O$ values across all taxa for each site. Next, we assigned each site to successive time bins of equal duration spanning the Pleistocene. We examined time bins under three geochronological scenarios related to the range of ages available for each site: (i) the minimum age of the site; (ii) the median age; and (iii) the maximum age. The number of time bins equalled the smallest division of the Quaternary that included at least one site in each bin. This resulted in 7 bins of 321-thousand-year (kyr) duration for minimum ages; 6 bins of 428 kyr for median age; and 5 bins of 513.8 kyr for maximum ages. We applied a locally weighted scatterplot smoothing spline[90,91] with a smoothing factor set at 0.9. The 95% confidence interval for the curve was based on 999 random replicates using resampling of residuals[89]. We compared our results to the Lisiecki Raymo benthic oxygen isotope stack[92], adjusted to the same temporal scale.

Most sites in Southeast Asia are derived from Late Pleistocene cave deposits (so there is unevenness in temporal sampling across the Quaternary) and/or they have poor constraints on their geological ages. At the extreme, geochronological constraints of these vertebrate deposits make it impossible to exclude the possibility that the fossils are sampling dry or wet states in some unexpected way, such that the patterns we observe could represent artefacts of taphonomic or sampling biases rather than broad environmental changes. Taphonomic bias could result from a restriction of fossil accumulation in caves to dry phases, as has been observed in South Africa[93]. Sampling bias could include the collection or analysis of only particular taxa from deposits. However, the possibility that the pattern we observe is artefactual can be discounted for several reasons. First, regarding taphonomy, low $\delta^{13}C$ values are recovered from samples from both cave and open-air sites (for example, Baxian and Cipeundeuy, respectively) and, equally, higher $\delta^{13}C$ values are also recovered from both types of sites (for example, Pha Bong and Khok Sung, respectively). Regarding sampling, several taxa—including the most commonly represented taxa in our dataset (that is, bovids and cervids)—span the range of $\delta^{13}C$ values of rainforest and savannah. Third, taphonomic and sampling biases would need to be structured in such a way that they provide a peak in $\delta^{13}C$ values at the beginning of the Middle Pleistocene. There are no structural biases in Middle Pleistocene sites that would differentiate them from Early and Late Pleistocene sites in this way. More importantly, the patterns we observe are fully consistent with major climatic changes in Southeast Asia reported by other proxies.

The climate in Southeast Asia is governed by the position of the intertropical convergence zone (ITCZ), which determines where precipitation from the East Asian and the Australian–Indonesian monsoons occurs[94]. Changes in the position of the ITCZ during the Pleistocene have substantially affected regional precipitation patterns and vegetation. The Mid-Pleistocene transition initiated high-amplitude 100,000-year glacial–interglacial cycles that were accompanied by heightened Asian aridity and monsoonal intensity[24], corresponding with the peak in our $\delta^{13}C_{diet}$ values. Following this, at the Mid-Brunhes event between MIS 13 and 11, interglacial conditions in high latitudes became warmer and more comparable to Holocene conditions[95]. However, cave speleothem records from Southeast Asia indicate that neither ITCZ activity nor its position responded to this event[96,97], although variable interglacial conditions were recorded. However, major changes to the ITCZ are observed following deglaciations, at which time environmental changes linked to the Earth's precession cycle and insolation intensity shifted and trapped the ITCZ in a southern position; this precipitated millennia-long intervals of reduced monsoon rainfall[96,97].

Decreasing trends in global glacial ice volume during the Late Pleistocene correspond to decreasing maximum peaks in oxygen isotopes over successive interglacial periods, which explains the decrease in drier conditions that we observe during this time. This would have been accentuated from about 400 ka by the initiation of Sunda shelf subsidence[25]. This reinforces the idea that the broad trends we observe in Southeast Asian vegetation were driven by global-scale climatic changes and regional-scale geological events. Nevertheless, such events can produce variable conditions locally: for example, the distribution of rainfall in Southeast Asia today is strongly dependent on topographical relief as well as the position of the ITCZ[94]. This can cause local-scale (temporal and/or spatial) environmental heterogeneity that may not be congruent with the larger-scale patterns we observe. For example, some palaeo-ecological records show that patches of both savannah and rainforest were present in Southeast Asia during the Late Pleistocene[98–105]. However, their effect on hominin and mammal biogeography must be understood in broader temporal and spatial environmental contexts. Only palaeo-ecological records such as ours provide direct insights into the environments that were actually used by mammals, as these records come from the animals themselves rather than via indirect proxies.

For canopy-specific analyses, herbivores with $\delta^{13}C$ values less than −23‰ were considered to belong to the browsing trophic group[22]. Browsers were further subdivided into subcanopy (below −32‰ $\delta^{13}C$), mid-canopy (−32 to −29‰ $\delta^{13}C$) and top-canopy browsers (−29 to −25.6‰ $\delta^{13}C$) (derived from ref. [21]). Stable oxygen values for these subdivisions were examined to determine forest stratification, with higher $\delta^{18}O$ values being predicted to occur in top-canopy folivores, and lower $\delta^{18}O$ values in subcanopy browsers[23].

Analysis of changes in isotopes across mammalian orders and trophic groups proceeded in two concurrent steps: between the same order over different periods, and between different orders in the same period. Summary statistics for the $\delta^{13}C$ and $\delta^{18}O$ values for each of these is provided in Extended Data Table 6. Statistical significance was assessed

via Kruskal–Wallis test with differences deemed significant at $\alpha = 0.05$. Changes across orders are illustrated in Extended Data Fig. 4.

To assess the relationship between extinction risk and environmental preference, we determined the conservation status for each taxon confidently identified to species from the International Union for Conservation of Nature (IUCN) Red List of Threatened Species[106]. We determined extinction times for Southeast Asian megafauna through an extensive literature survey, with sites and dates listed in Table 1 sourced from refs. [67,71,73,107–118]. We calculated whether a correlation between conservation risk and extinction status, and $\delta^{13}C$ and $\delta^{18}O$ values, existed, using Kendall's τ with significance assessed at $\alpha = 0.05$. To examine current threats to Southeast Asian mammal biodiversity, we examined the same dataset but removed extinct species from the list.

Reporting summary

Further information on research design is available in the Nature Research Reporting Summary linked to this paper.

Data availability

All accession numbers, and data generated and used during this study, are included in the Article and its Supplementary Information.

33. Craig, H. The geochemistry of the stable carbon isotope. *Geochim. Cosmochim. Acta* **3**, 53–92 (1953).
34. Smith, B. N. & Epstein, S. Two categories of $^{13}C/^{12}C$ ratios for higher plants. *Plant Physiol.* **47**, 380–384 (1971).
35. Tieszen, L. L. Natural variations in the carbon isotope values of plants: implications for archaeology, ecology, and paleoecology. *J. Archaeol. Sci.* **18**, 227–248 (1991).
36. Sponheimer, M. et al. Do "savanna" chimpanzees consume C_4 resources? *J. Hum. Evol.* **51**, 128–133 (2006).
37. Sponheimer, M. et al. Isotopic evidence of early hominin diets. *Proc. Natl Acad. Sci. USA* **110**, 10513–10518 (2013).
38. Codron, J. et al. Stable isotope series from elephant ivory reveal lifetime histories of a true dietary generalist. *Proc. R. Soc. Lond. B* **279**, 2433–2441 (2012).
39. Crowley, B. E. et al. Extinction and ecology retreat in a community of primates. *Proc. R. Soc. Lond. B* **279**, 3597–3605 (2012).
40. Farquhar, G. D., Ehleringer, J. R. & Hubick, K. T. Carbon isotope discrimination and photosynthesis. *Annu. Rev. Plant Physiol. Plant Mol. Biol.* **40**, 503–537 (1989).
41. van der Merwe, N. J. & Medina, E. The canopy effect, carbon isotope ratios and foodwebs in Amazonia. *J. Archaeol. Sci.* **18**, 249–259 (1991).
42. Pearcy, R. W. & Pfitsch, W. A. Influence of sunflecks on the $\delta^{13}C$ of *Adenocaulon bicolor* plants occurring in contrasting forest understory microsites. *Oecologia* **86**, 457–462 (1991).
43. Bonafini, M., Pellegrini, M., Ditchfield, P. & Pollard A. M. Investigation of the 'canopy effect' in the isotope ecology of temperate woodlands. *J. Archaeol. Sci.* **40**, 3926–3935 (2013).
44. Ehleringer, J. R., Rundel, P. W. & Nagy, K. A. Stable isotopes in physiological ecology and food web research. *Trends Ecol. Evol.* **1**, 42–45 (1986).
45. van der Merwe, N. J. & Medina, E. Photosynthesis and $^{13}C/^{12}C$ ratios in Amazonian rainforests. *Geochim. Cosmochim. Acta* **53**, 1091–1094 (1989).
46. Ometto, J. P. H. B. et al. The stable carbon and nitrogen isotopic composition of vegetation in tropical forests of the Amazon Basin, Brazil. *Biogeochemistry* **79**, 251–274 (2006).
47. Gonfiantini, R., Gratziu, S. & Tongiorgi, E. in *Isotopes and Radiation in Soil Plant Nutrition Studies (Technical Report Series No. 206)* (ed. Joint FAO/IAEA Division of Atomic Energy in Agriculture) 405–410 (Isotope Atomic Energy Commission, 1965).
48. Flanagan, L. B., Comstock, J. P. & Ehleringer, J. R. Comparison of modelled and observed environmental influences on the stable oxygen and hydrogen isotope composition of leaf water in *Phaseolus vulgaris* L. *Plant Physiol.* **96**, 588–596 (1991).
49. Yakir, D., Berry, J. A., Giles, L. & Osmond, C. B. Isotopic heterogeneity of water in transpiring leaves: Identification of the component that controls the $\delta^{18}O$ of atmospheric O_2 and CO_2. *Plant Cell Environ.* **17**, 73–80 (1994).
50. Sheshshayee, M. S. et al. Oxygen isotope enrichment ($\Delta^{18}O$) as a measure of time-averaged transpiration rate. *J. Exp. Bot.* **56**, 3033–3039 (2005).
51. Buchmann, N. & Ehleringer, J. R. CO_2 concentration profiles, and carbon and oxygen isotopes in C_3 and C_4 crop canopies. *Agric. For. Meteorol.* **89**, 45–58 (1998).
52. Buchmann, N., Guehl, J. M., Barigah, T. S. & Ehleringer, J. R. Interseasonal comparison of CO_2 concentrations, isotopic composition, and carbon dynamics in an Amazonian rainforest (French Guiana). *Oecologia* **110**, 120–131 (1997).
53. da Silveira, L., Sternberg, L., Mulkey, S. S. & Joseph Wright, S. Oxygen isotope ratio stratification in a tropical moist forest. *Oecologia* **81**, 51–56 (1989).
54. McCarroll, D. & Loader, N. J. in *Isotopes in Palaeonvironmental Research* (ed. Leng, M. J.) 67–116 (Springer, 2006).
55. Carter, M. L. & Bradbury, M. W. Oxygen isotope ratios in primate bone carbonate reflect amount of leaves and vertical stratification in the diet. *Am. J. Primatol.* **78**, 1086–1097 (2016).
56. Kohn, M. J., Schoeninger, M. J. & Valley, J. W. Herbivore tooth oxygen isotope compositions: effects of diet and physiology. *Geochim. Cosmochim. Acta* **60**, 3889–3896 (1996).
57. Levin, N. E., Cerling, T. E., Passey, B. H., Harris, J. M. & Ehleringer, J. R. A stable isotope aridity index for terrestrial environments. *Proc. Natl Acad. Sci. USA* **103**, 11201–11205 (2006).
58. Lee-Thorp, J. et al. Isotopic evidence for an early shift to C_4 resources by Pliocene hominins in Chad. *Proc. Natl Acad. Sci. USA* **109**, 20369–20372 (2012).
59. Roberts, P. et al. Fruits of the forest: Human stable isotope ecology and rainforest adaptations in Late Pleistocene and Holocene (<36 to 3 ka) Sri Lanka. *J. Hum. Evol.* **106**, 102–118 (2017).
60. Snoeck, C. & Pellegrini, M. Comparing bioapatite carbonate pre-treatments for isotopic measurements: part 1 – impact on structure and chemical composition. *Chem. Geol.* **417**, 394–403 (2015).
61. Pellegrini, M. & Snoeck, C. Comparing bioapatite carbonate pre-treatments for isotopic measurements: part 2 – impact on carbon and oxygen isotope compositions. *Chem. Geol.* **420**, 88–96 (2016).
62. Jiang, Q. Y., Zhao, L. X. & Hu, Y. W. Variations of fossil enamel bioapatite caused by different preparation and measurement protocols: a case study of *Gigantopithecus* fauna. *Vertebrata PalAsiatica* **58**, 159–168 (2020).
63. Pushkina, D., Bocherens, H., Chaimanee, Y. & Jaeger, J. J. Stable carbon isotope reconstructions of diet and paleoenvironment from the late Middle Pleistocene Snake Cave in Northeastern Thailand. *Naturwissenschaften* **97**, 299–309 (2010).
64. Ma, J. et al. Isotopic evidence of foraging ecology of Asian elephant (*Elephas maximus*) in South China during the Late Pleistocene. *Quat. Int.* **443**, 160–167 (2017).
65. Ma, J. et al. Ecological flexibility and differential survival of Pleistocene *Stegodon orientalis* and *Elephas maximus* in mainland southeast Asia revealed by stable isotope (C, O) analysis. *Quat. Sci. Rev.* **212**, 33–44 (2019).
66. Bacon, A. M. et al. Nam Lot (MIS 5) and Duoi U'Oi (MIS 4) Southeast Asian sites revisited: zooarchaeological and isotopic evidences. *Palaeogeogr. Palaeoclimatol. Palaeoecol.* **512**, 132–144 (2018).
67. Bacon, A. M. et al. Testing the savannah corridor hypothesis during MIS2: the Boh Dambang hyena site in southern Cambodia. *Quat. Int.* **464**, 417–439 (2018).
68. Suraprasit, K. et al. Late Middle Pleistocene ecology and climate in northeastern Thailand inferred from the stable isotope analysis of Khok Sung herbivore tooth enamel and the land mammal cenogram. *Quat. Sci. Rev.* **193**, 24–42 (2018).
69. Suraprasit, K. et al. New fossil and isotope evidence for the Pleistocene zoogeographic transition and hypothesized savanna corridor in peninsular Thailand. *Quat. Sci. Rev.* **221**, 105861 (2019).
70. Bocherens, H. et al. Flexibility of diet and habitat in Pleistocene South Asian mammals: implications for the fate of the giant fossil ape *Gigantopithecus*. *Quat. Int.* **434**, 148–155 (2017).
71. Puspaningrum, M. R. et al. Isotopic reconstruction of proboscidean habitats and diets on Java since the Early Pleistocene: implications for adaptation and extinction. *Quat. Sci. Rev.* **228**, 106007 (2020).
72. Janssen, R. et al. Tooth enamel stable isotopes of Holocene and Pleistocene fossil fauna reveal glacial and interglacial paleoenvironments of hominins in Indonesia. *Quatern. Sci. Rev. (Singap.)* **144**, 145–154 (2016).
73. Wang, W. et al. Sequence of mammalian fossils, including hominoid teeth, from the Bubing Basin caves, South China. *J. Hum. Evol.* **52**, 370–379 (2007).
74. Nelson, S. V. The paleoecology of early Pleistocene *Gigantopithecus blacki* inferred from isotopic analyses. *Am. J. Phys. Anthropol.* **155**, 571–578 (2014).
75. Qu, Y. et al. Preservation assessments and carbon and oxygen isotopes analysis of tooth enamel of *Gigantopithecus blacki* and contemporary animals from Sahne Cave, Chongzuo, South China during the Early Pleistocene. *Quat. Int.* **354**, 52–58 (2014).
76. Uno, K. T. et al. Late Miocene to Pliocene carbon isotope record of differential diet change among East African herbivores. *Proc. Natl Acad. Sci. USA* **108**, 6509–6514 (2011).
77. LeGeros, R. Z. *Calcium Phosphates in Oral Biology and Medicine (Monographs in Oral Science 15)* (1991).
78. Lee-Thorp, J. A. On isotopes and old bones. *Archaeometry* **50**, 925–950 (2008).
79. Friedli, H. et al. Ice core record of the $^{13}C/^{12}C$ ratio of atmospheric CO_2 in the past two centuries. *Nature* **324**, 237–238 (1986).
80. Graven, H. et al. Compiled records of carbon isotopes in atmospheric CO_2 for historical simulations in CMIP6. *Geosci. Model Dev.* **10**, 4405–4417 (2017).
81. Ambrose, S. H. & Norr, L. in *Prehistoric Human Bone* 1–37 (Springer, Berlin, Heidelberg, 1993).
82. Cerling, T. E. & Harris, J. M. Carbon isotope fractionation between diet and bioapatite in ungulate mammals and implications for ecological and paleoecological studies. *Oecologia* **120**, 347–363 (1999).
83. Crowley, B. E. et al. Stable carbon and nitrogen isotope enrichment in primate tissues. *Oecologia* **164**, 611–626 (2010).
84. Lee-Thorp, J. A., Sealy, J. C. & van der Merwe, N. J. Stable carbon isotope ratio differences between bone collagen and bone apatite, and their relationship to diet. *J. Archaeol. Sci.* **16**, 585–599 (1989).
85. Kellner, C. M. & Schoeninger, M. J. A simple carbon isotope model for reconstructing prehistoric human diet. *Am. J. Phys. Anthropol.* **133**, 1112–1127 (2007).
86. Karasov, W. H. & Douglas, A. E. Comparative digestive physiology. *Compr. Physiol.* **3**, 741–783 (2013).
87. Ley, R. E. et al. Evolution of mammals and their gut microbes. *Science* **320**, 1647–1651 (2008).
88. Furness, J. B., Cottrell, J. J. & Bravo, D. M. Comparative gut physiology symposium: comparative physiology of digestion. *J. Anim. Sci.* **93**, 485–491 (2015).
89. Hammer, Ø., Harper, D. A. & Ryan, P. D. PAST: paleontological statistics software package for education and data analysis. *Palaeontol. Electronica* **4**, 9 (2001).
90. Cleveland, W. S. Robust locally weighted fitting and smoothing scatterplots. *J. Am. Stat. Assoc.* **74**, 829–836 (1979).
91. Cleveland, W. S. A program for smoothing scatterplots by robust locally weighted fitting. *Am. Stat.* **35**, 54 (1981).
92. Lisiecki, L. E., & Raymo M. E. A. Pliocene–Pleistocene stack of 57 globally distributed benthic $\delta^{18}O$ records. *Paleoceanogr.* **20**, PA1003 (2005).

93. Pickering, R. et al. U–Pb-dated flowstones restrict South African early hominin record to dry climate phases. *Nature* **565**, 226–229 (2019).
94. Chuan, G. K. in *The Physical Geography of Southeast Asia* (ed. Gupta, A.) 80–93 (Oxford Univ. Press, 2005).
95. Candy, I. et al. Pronounced warmth during early Middle Pleistocene interglacials: investigating the Mid-Brunhes Event in the British terrestrial sequence. *Earth Sci. Rev.* **103**, 183–196 (2010).
96. Meckler, A. N., Clarkson, M. O., Cobb, K. M., Sodemann, H. & Adkins, J. F. Interglacial hydroclimate in the tropical west Pacific through the Late Pleistocene. *Science* **336**, 1301–1304 (2012).
97. Cheng, H. et al. The Asian monsoon over the past 640,000 years and ice age terminations. *Nature* **534**, 640–646 (2016).
98. Maloney, B. K. & McCormac, F. G. Palaeoenvironments of north Sumatra: a 30,000 year old pollen record from Pea Bullok. *Bull. Indo-Pacific Prehist. Ass.* **14**, 73–82 (1996).
99. van der Kaars, W. A. & Dam, M. A. C. A. 135,000-year record of vegetational and climatic change from the Bandung area, West-Java, Indonesia. *Palaeogeogr. Palaeoclimatol. Palaeoecol.* **117**, 55–72 (1995).
100. van der Kaars, W. A. & Dam, M. A. C. Vegetation and climate change in West-Java, Indonesia during the last 135,000 years. *Quat. Int.* **37**, 67–71 (1997).
101. Wurster, C. M. et al. Forest contraction in north equatorial Southeast Asia during the last glacial period. *Proc. Natl Acad. Sci. USA* **107**, 15508–15511 (2010).
102. Wurster, C. M., Rifai, H., Zhou, B., Haig, J. & Bird, M. I. Savanna in equatorial Borneo during the Late Pleistocene. *Sci. Rep.* **9**, 6392 (2019).
103. Dubois, N. et al. Indonesian vegetation response to changes in rainfall seasonality over the past 25,000 years. *Nat. Geosci.* **7**, 513–517 (2014).
104. Sun, X. et al. Deep-sea pollen from the South China Sea: Pleistocene indicators of East Asian monsoon. *Mar. Geol.* **201**, 97–118 (2003).
105. Yu, S. et al. Pollen record in the northwestern continental shelf of the South China Sea in the past 82 ka: paleoenvironmental changes in the last glacial period. *J. Asian Earth Sci.* **199**, 104457 (2020).
106. IUCN. *The IUCN Red List of Threatened Species.* Version 2019-3 http://www.iucnredlist.org (accessed 6 November 2019).
107. Yang, D. et al. *Researches of* Ailuropoda–Stegodon *Fauna from Gulin China* (in Chinese with English abstract) (Chongqing, 1995).
108. Turvey, S. T. et al. Holocene survival of Late Pleistocene megafauna in China: a critical review of the evidence. *Quat. Sci. Rev.* **76**, 156–166 (2013).
109. Jin, C. et al. Chronological sequence of the early Pleistocene *Gigantopithecus* faunas from cave sites in the Chongzuo, Zuojiang River area, South China. *Quat. Int.* **354**, 4–14 (2014).
110. Rizal, Y. et al. Last appearance of *Homo erectus* at Ngandong, Java, 117,000–108,000 years ago. *Nature* **577**, 381–385 (2020).
111. Joordens, J. C. et al. *Homo erectus* at Trinil on Java used shells for tool production and engraving. *Nature* **518**, 228–231 (2015).
112. Zhang, Y. et al. New 400–320 ka *Gigantopithecus blacki* remains from Hejiang Cave, Chongzuo City, Guangxi, South China. *Quat. Int.* **354**, 35–45 (2014).
113. Han, D. & Xu, C. in *Palaeoanthropology and Palaeolithic Archaeology in the People's Republic of China* (eds Rukang, W. & Olsen, J. W.) 267–289 (Academic, 1985).
114. Lu, C., Xu, X. & Sun, X. Re-dating Changyang Cave in Hubei Province, southern China. *Quat. Int.* **537**, 1–8 (2020).
115. van den Bergh, G. D. et al. The Early Pleistocene terrestrial vertebrate faunal sequence of Java, Indonesia. *J. Vert. Paleol.* Abstract 210 (2019).
116. Dong, W. et al. New materials of Early Pleistocene *Sus* from Sanhe Cave, Chongzuo, Guangxi, South China. *Acta Anthropol. Sin.* **32**, 63–76 (2013).
117. Shao, Q. et al. Coupled ESR and U-series dating of early Pleistocene *Gigantopithecus* faunas at Mohui and Sanhe Caves, Guangxi, southern China. *Quat. Geochronol.* **30**, 524–528 (2015).
118. Rink, W. J., Wei, W., Bekken, D. & Jones, H. L. Geochronology of *Ailuropoda–Stegodon* fauna and *Gigantopithecus* in Guangxi Province, southern China. *Quat. Res.* **69**, 377–387 (2008).
119. Wang, Y., Jin, C. Z. & Mead, J. I. New remains of *Sinomastodon yangziensis* (Proboscidea, Gomphotheriidae) from Sanhe karst cave, with discussion on the evolution of Pleistocene *Sinomastodon* in South China. *Quat. Int.* **339–340**, 90–96 (2014).
120. Duval, M. et al. Direct ESR dating of the Pleistocene vertebrate assemblage from Khok Sung locality, Nakhon Ratchasima Province, Northeast Thailand. *Pal. Electr.* **22**, 1–25 (2019).
121. Li, H., Li, C. & Kuman, K. Longgudong, an Early Pleistocene site in Jianshi, South China, with stratigraphic association of human teeth and lithics. *Sci. China Earth Sci.* **60**, 452–462 (2017).
122. Bacon, A. M. et al. Late Pleistocene mammalian assemblages of Southeast Asia: new dating, mortality profiles and evolution of the predator–prey relationships in an environmental context. *Palaeogeogr. Palaeoclimatol. Palaeoecol.* **422**, 101–127 (2015).
123. Westaway, K. E. et al. Age and biostratigraphic significance of the Punung rainforest fauna, East Java, Indonesia, and implications for *Pongo* and *Homo*. *J. Hum. Evol.* **53**, 709–717 (2007).
124. Matsu'ura, S. et al. Age control of the first appearance datum for Javanese *Homo erectus* in the Sangiran area. *Science* **367**, 210–214 (2020).
125. Sun, L. et al. Magnetochronological sequence of the early Pleistocene *Gigantopithecus* faunas in Chongzuo, Guangxi, southern China. *Quat. Int.* **354**, 15–23 (2014).
126. Esposito, M., Reyss, J. L., Chaimanee, Y. & Jaeger, J. J. U-series dating of fossil teeth and carbonates from Snake Cave, Thailand. *J. Archaeol. Sci.* **29**, 341–349 (2002).
127. Storm, P. et al. U-series and radiocarbon analyses of human and faunal remains from Wajak, Indonesia. *J. Hum. Evol.* **64**, 356–365 (2013).

Acknowledgements We thank E. Hoeger, R. Voss, L. Kok Peng, A. van Heteren, J. Cuisin, V. Nicolas, G. Véron, J. Lesur and C. Lefèvre for allowing access to specimens under their care, N. Boivin and the Max Planck Society for support and J. Ilgner, M. Lucas, E. Perruchini and S. Marzo for their assistance with analysis of the samples. The map in Fig. 1 was provided by CartoGIS Services, ANU College of Asia and the Pacific, The Australian National University; we thank S. Potter and K. Pelling for providing the map. This research was supported by an Australian Research Council Future Fellowship to J.L. (FT160100450). P.R. was funded by the Max Planck Society and the European Research Council (ERC) under the European Union's Horizon 2020 research and innovation programme (grant agreement no. 850709).

Author contributions J.L. conceived this research and conducted the statistical analyses. P.R. performed the stable isotope analyses. Both authors contributed equally to study design, data acquisition, interpretation of data and the writing of the final manuscript.

Competing interests The authors declare no competing interests.

Additional information

Supplementary information is available for this paper at https://doi.org/10.1038/s41586-020-2810-y.

Correspondence and requests for materials should be addressed to J.L. or P.R.

Peer review information *Nature* thanks Thure Cerling and the other, anonymous, reviewer(s) for their contribution to the peer review of this work. Peer reviewer reports are available.

Reprints and permissions information is available at http://www.nature.com/reprints.

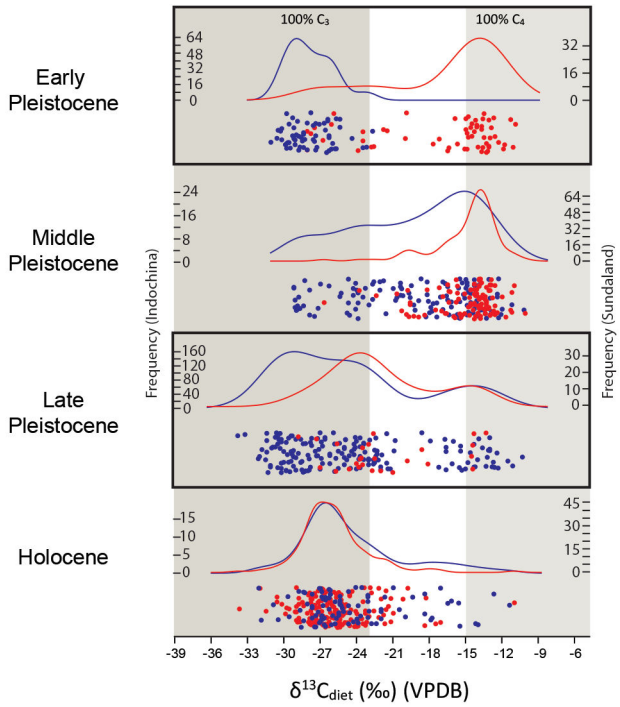

Extended Data Fig. 1 | Distribution of $\delta^{13}C$ values across the Quaternary. Distribution is shown with a jitter plot and corresponding kernel density for Indochina (blue) and Sundaland (red). Kernel densities are exaggerated vertically, such that the peaks for both provinces are equal. Shaded boxes represent the division between $\delta^{13}C$ values associated with forests (left) and grasslands (right).

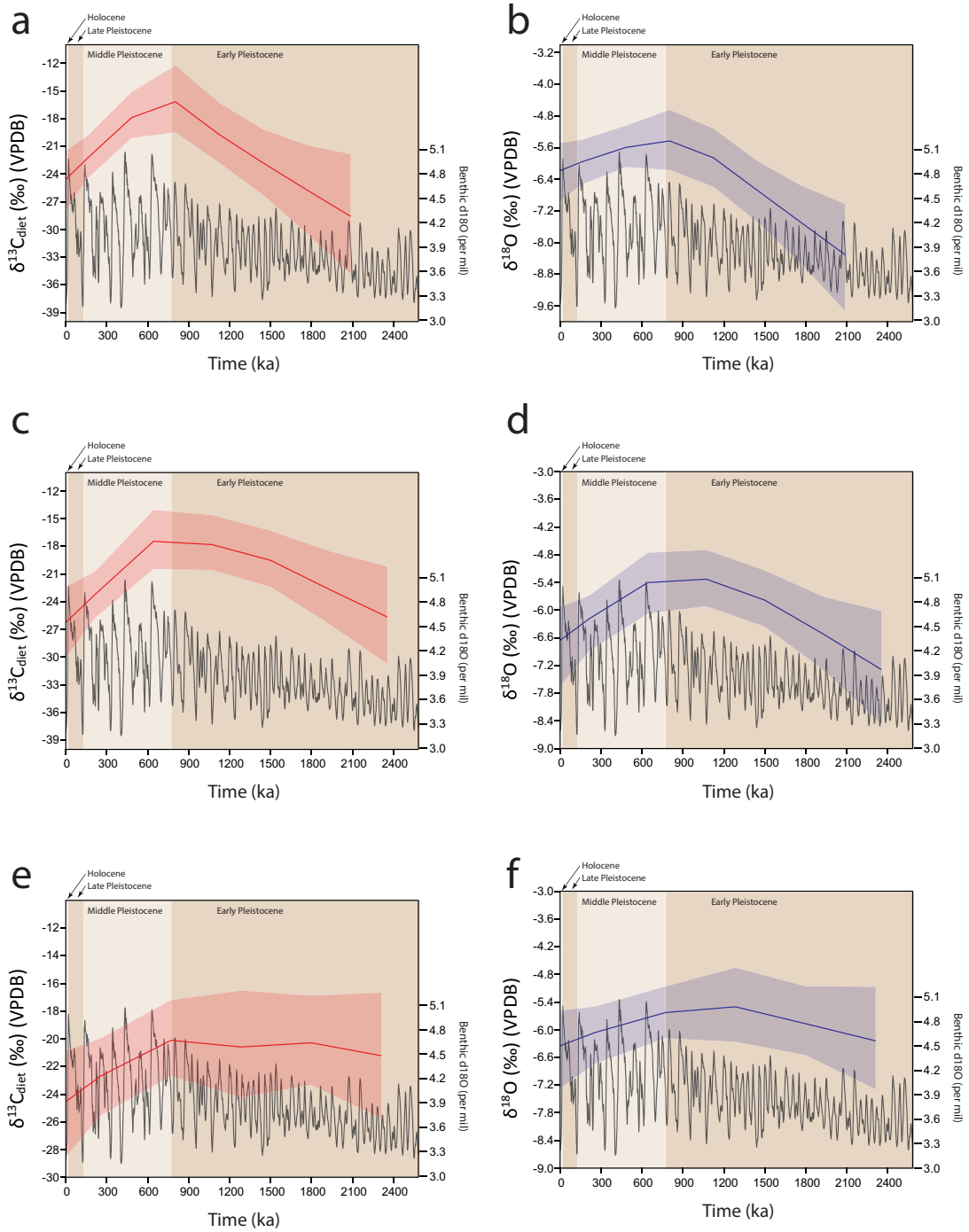

Extended Data Fig. 2 | Temporal trends of $\delta^{13}C$ and $\delta^{18}O$ values under different geochronological scenarios. a, $\delta^{13}C$ values assuming minimum age for each site. **b**, $\delta^{18}O$ values assuming minimum age for each site. **c**, $\delta^{13}C$ values assuming median age for each site. **d**, $\delta^{18}O$ values assuming median age for each site. **e**, $\delta^{13}C$ values assuming maximum age for each site. **f**, $\delta^{18}O$ values assuming maximum age for each site. Each panel is shown relative to the Lisiecki Raymo benthic oxygen-isotope stack. The 95% confidence interval for each curve was based on 999 random replicates using resampling of residuals.

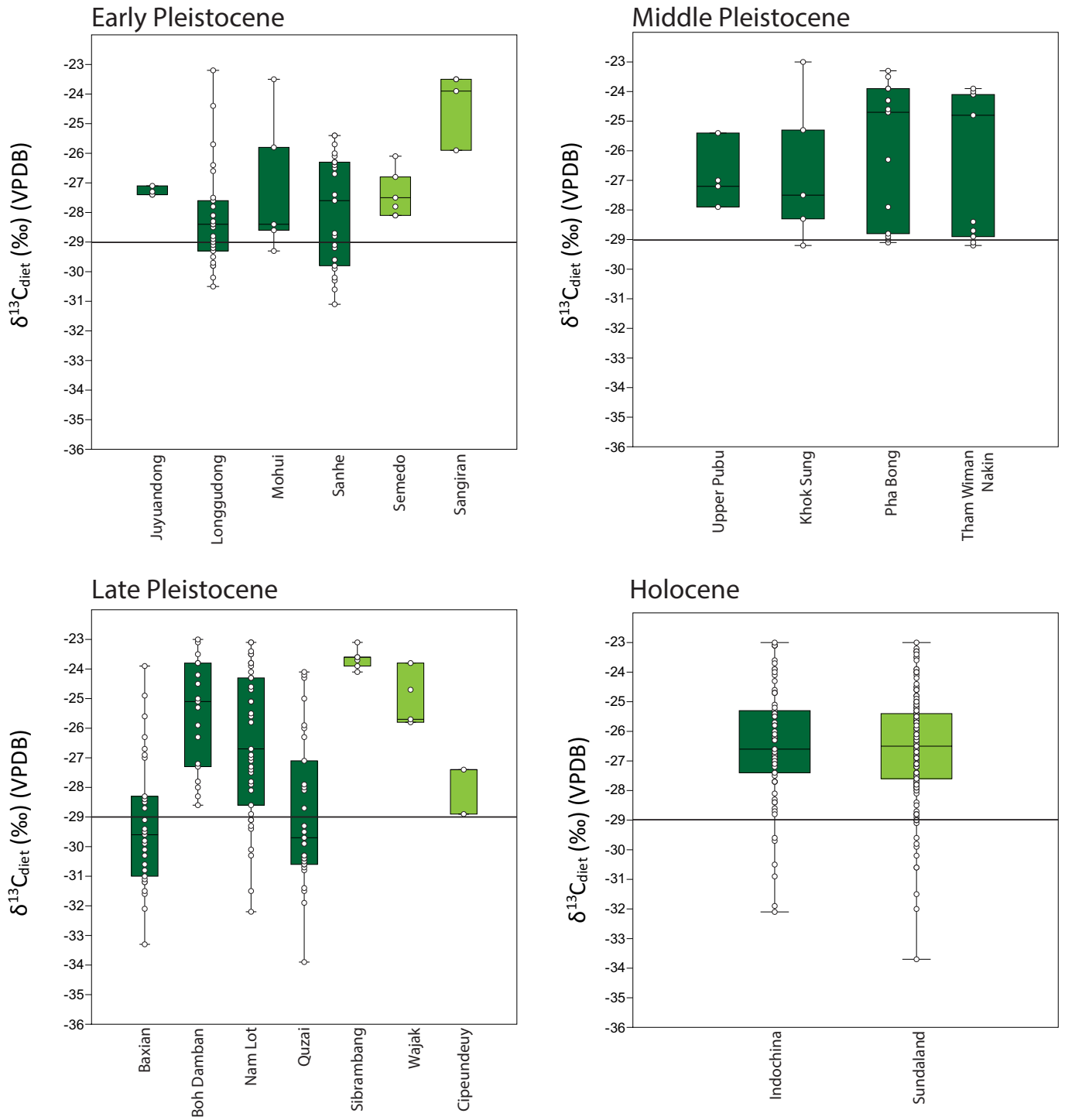

Extended Data Fig. 3 | Distribution of $\delta^{13}C$ values for browsers across fossil sites through Southeast Asia. Indochina, dark green; Sundaland, light green. Horizontal line represents the −29‰ zone that indicates the beginning of subcanopy and closed-canopy environments. The long lower whiskers in the box and whisker plot, which indicate a very negatively skewed distribution, are most closely associated with highly stratified forests. The boxes show the median and the lower (25%) and upper (75%) quartiles; the whiskers encompass the minimum and maximum values. Independent sample sizes: Juyuandong, $n = 4$; Longudong, $n = 26$; Mohui, $n = 5$; Sanhe, $n = 25$; Semedo, $n = 6$; Sangiran, $n = 4$; Upper Pubu, $n = 4$; Khok Sung, $n = 5$; Pha Bong, $n = 15$; Tham Wiman Nakin, $n = 10$; Baxian, $n = 32$; Boh Damban, $n = 18$; Nam Lot, $n = 39$; Quzai, $n = 32$; Sibrambang, $n = 6$; Wajak, $n = 4$; Cipeundeuy, $n = 2$; Indochina, $n = 74$; and Sundaland, $n = 158$.

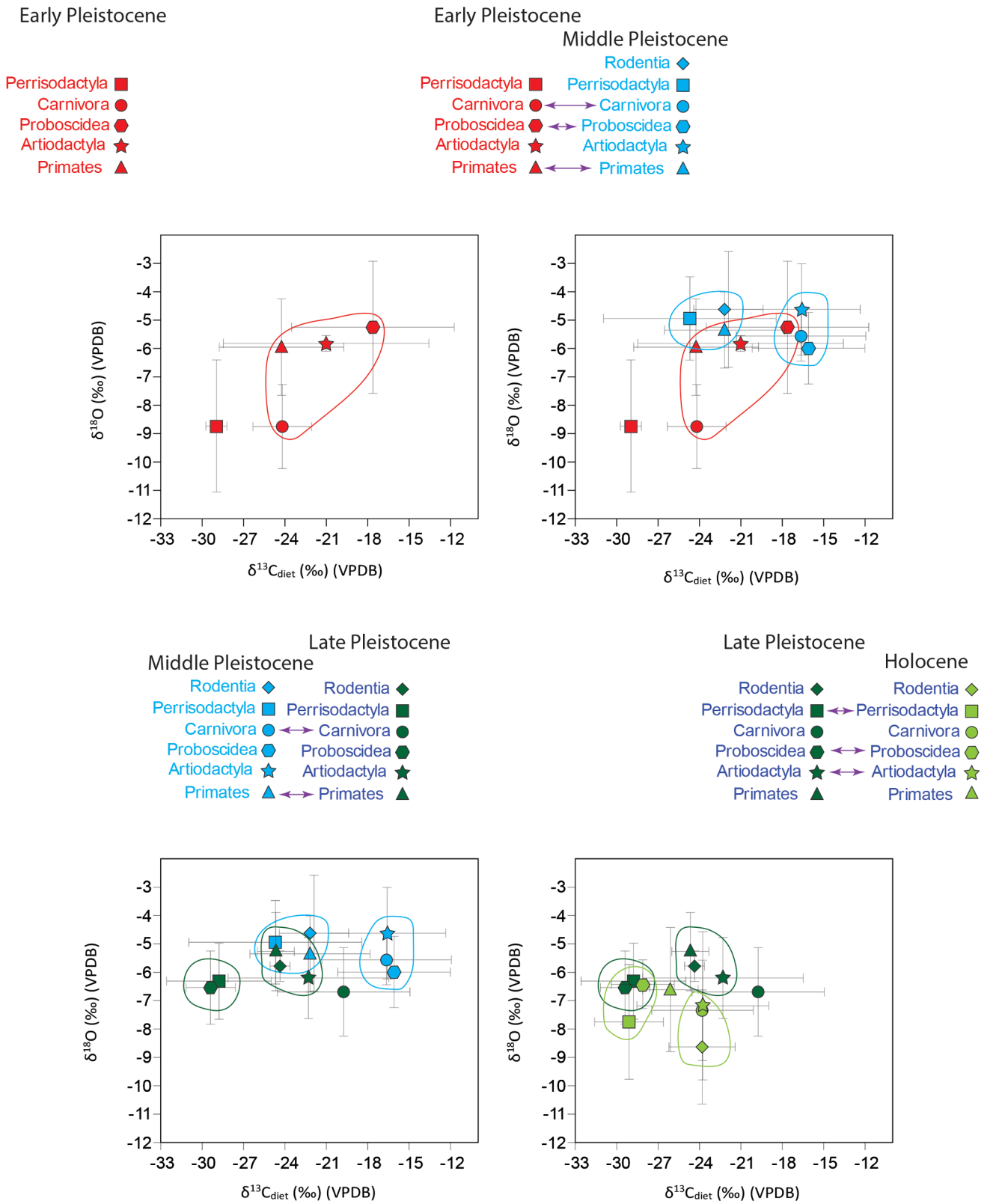

Extended Data Fig. 4 | Changes in mean $\delta^{13}C$ and $\delta^{18}O$ values for mammals classified at the ordinal level. Continuities (non-significant differences in mean) of $\delta^{13}C$ values within orders between epochs are illustrated with arrows at the top of each plot. Continuities between orders in a single epoch are illustrated with circles bounding similar $\delta^{13}C$ means. Variation within orders and epochs is indicated at 1 s.d.

Extended Data Table 1 | Sites included in the analyses with corresponding sources for the isotope data

Site Number	Locality	Biogeographical Province	Age	Source	N
1	Baxian	Indochina	Late Pleistocene	ref[64]	32
2	Boh Dambang	Indochina	Late Pleistocene	ref[67]	52
3	Bubin Basin Caves (Mohui and Upper Pubu)	Indochina	Early and Middle Pleistocene	ref[73]	9
4	Bumiayu	Sundaland	Early Pleistocene	ref[71]	8
5	China?	Indochina	Pleistocene	ref[70]	6
6	“Chinese cave from Dr Kamal”	Indochina	Pleistocene	ref[70]	3
7	Cipendeuy	Sundaland	Late Pleistocene	ref[71]	3
8	Cirebon	Sundaland	Early Pleistocene	ref[71]	1
9	Hoekgrot	Sundaland	Holocene	ref[72]	4
10	Juyuandong	Indochina	Early Pleistocene	ref[74]	4
11	Kedung Brubus	Sundaland	Middle Pleistocene	ref[71]	10
12	Khok Sung	Indochina	Middle Pleistocene	ref[68]	38
13	Longgudong	Indochina	Early Pleistocene	ref[74]	27
14	Nam Lot	Indochina	Late Pleistocene	ref[66]	51
15	Ngandong	Sundaland	Middle Pleistocene	ref[71]	10
16	Padang Caves	Sundaland	Pleistocene	ref[72]	15
17	Pha Bong	Indochina	Middle Pleistocene	ref[70]	53
18	Punung	Indochina	Late Pleistocene	ref[72]	3
19	Quzai	Indochina	Late Pleistocene	ref[65]	40
20	Sambungmacan	Sundaland	Early Pleistocene	ref[71]	1
21	Sangiran	Sundaland	Early and Middle Pleistocene	refs[71,72]	61
22	Sanhe Cave	Indochina	Early Pleistocene	ref[75]	25
23	Semedo	Sundaland	Early and Middle Pleistocene	ref[71]	10
24	Sibrambang	Sundaland	Late Pleistocene	ref[72]	10
25	Su Bang	Sundaland	Middle Pleistocene	ref[71]	4
26	Sunggu, Blora	Sundaland	Middle Pleistocene	ref[71]	1
27	Tham Wiman Nakin	Indochina	Middle Pleistocene	ref[71]	28
28	Trinil	Sundaland	Middle Pleistocene	ref[72]	64
29	Wajak	Sundaland	Late Pleistocene	ref[72]	10
30	Yai Ruak	Sundaland	Pleistocene	Ref[69]	10
	Recent and modern	Indochina and Sundaland	Holocene	refs[63,70,71]	51

Data are from refs. [63–75].

Extended Data Table 2 | Univariate statistics for each geological subepoch and biogeographical province

	Holocene		Late Pleistocene		Middle Pleistocene		Early Pleistocene	
	Sundaland	Indochina	Sundaland	Indochina	Sundaland	Indochina	Sundaland	Indochina
N	179	97	26	175	111	123	60	61
Min	-33.7	-32.1	-28.9	-33.9	-26.7	-29.2	-28.1	-31.1
Max	-11.0	-11.4	-13.4	-10.4	-10.1	-10.2	-10.9	-22.7
Mean	-25.8	-24.5	-21.7	-24.4	-14.9	-19.1	-16.7	-27.9
Std. Error	0.2	0.4	0.9	0.4	0.3	0.5	0.7	0.2
Variance	7.7	17.9	19.5	34.7	7.1	27.5	25.3	3.6
Std. Dev	2.8	4.2	4.4	5.9	2.7	5.2	5.0	1.9
Median	-26.2	-25.7	-23.0	-25.6	-14.1	-17.9	-14.6	-28.3
Q1	-27.5	-27.0	-24.3	-29.3	-15.8	-23.9	-20.0	-29.3
Q3	-24.8	-23.05	-18.6	-22.1	-13.3	-14.8	-13.3	-26.4
Skewness	1.3	1.1	0.6	0.8	-1.7	-0.5	-1.1	0.7
Kurtosis	5.0	1.0	-0.6	-0.5	4.0	-1.0	-0.1	0.1

Extended Data Table 3 | Univariate statistics for each geological subepoch and trophic group

	Holocene			Late Pleistocene			Middle Pleistocene			Early Pleistocene		
	Herbivore	Omnivore	Carnivore	Herbivore	Omnivore	Carnivore	Herbivore	Omnivore	Carnivore	Herbivore	Omnivore	Carnivore
N	270	38	15	149	38	14	207	20	7	101	19	1
Min	-33.7	-27.7	-29.7	-33.9	-26.7	-23.0	-29.2	-25.8	-19.6	-31.1	-25.9	-22.70
Max	-11.0	-14.2	-17.5	-11.2	-11.6	-10.4	-10.1	-13.0	-10.2	-10.9	-11.1	-22.70
Mean	-25.5	-23.5	-24.0	-25.3	-22.3	-16.2	-16.9	-20.4	-14.6	-23.0	-18.8	
Std. Error	0.2	0.4	1.0	0.5	0.5	1.2	0.3	0.7	1.1	0.7	1.2	
Variance	13.9	5.1	14.4	33.1	8.7	20.7	22.7	10.9	8.7	47.0	26.6	
Stand. Dev	3.8	2.3	3.8	5.8	2.9	4.5	4.8	3.2	2.9	6.9	5.2	
Median	-26.3	-24.0	-23.3	-27.1	-23.0	-14.2	-14.9	-20.4	-14.3	-26.4	-17.7	
Q1	-27.5	-24.9	-28.3	-29.6	-24.1	-22.5	-18.9	-23.7	-16.6	-28.7	-23.5	
Q3	-24.7	-22.0	-21.8	-23.3	-21.6	-12.9	-13.7	-18.2	-13.1	-14.6	-13.7	
Skewness	1.4	1.8	0.0	1.0	2.0	-0.7	-1.3	0.5	-0.3	0.5	0.1	
Kurtosis	2.8	6.7	-0.9	-0.2	4.7	-1.2	0.6	-0.4	0.9	-1.5	-1.6	

Extended Data Table 4 | Count data for Early and Middle Pleistocene herbivores and omnivores

	Herbivore		Omnivore	
Cluster	Early Pleistocene	Middle Pleistocene	Early Pleistocene	Middle Pleistocene
$\delta^{13}C > -20‰$	36	152	10	9
$\delta^{13}C < -20‰$	65	55	9	11

Extended Data Table 5 | Age ranges for fossil sites and the time bins to which they were allocated for each age modelling scenario

Site Name	Reported Age	Minimum (ka)	Median (ka)	Maximum (ka)	Bin (min)	Bin (med)	Bin (max)	Reference
Baxian	Early Late Pleistocene	11.7	70.35	129	1	1	1	ref[64]
Boh Dambang	18-25 ka	18	21.5	25	1	1	1	ref[67]
Mohui	11.8-19.1 Ma	1180	1545	1910	4	4	4	ref[117]
Upper Pubu	Late Pleistocene (<88 ka)	11.7	49.85	88	1	1	1	ref[118]
Bumiayu	Early Pleistocene (>1.5 Ma)	1500	2040	2580	5	5	5	van den Bergh et al. 2019 cited in ref[71]
Cipendeuy	35 +4.6/-2.9	32.6	35.5	40.1	1	1	1	ref[71]
Cirebon	Early Pleistocene	774	1677	2580	3	4	5	ref[71]
Hoekgrot	2.6-3.3 ka	2.6	2.95	3.3	1	1	1	Shutler et al. 2004 cited in ref[72]
Juyuandong	Early Early Pleistocene	1800	2190	2580	6	6	5	ref[119]
Kedung Brubus	700-800 ka	700	750	800	3	2	2	Mubroto et al. 1995 cited in ref[71]
Khok Sung	101-253 ka	101	177	253	1	1	1	ref[120]
Longgudong	Early Early Pleistocene (>2.14 Ma)	2140	2360	2580	7	6	5	ref[121]
Nam Lot	72-86 ka	72	79	86	1	1	1	ref[122]
Ngandong	108-117 ka	108	112.5	117	1	1	1	ref[110]
Pha Bong	Middle Pleistocene	129	451.5	774	1	2	2	ref[70]
Punung	115-143 ka	115	129	143	1	1	1	ref[123]
Quzai	Late Pleistocene	11.7	70.35	129	1	1	1	ref[65]
Sambungmacan	Early Pleistocene	774	1677	2580	3	4	5	ref[71]
Sangiran	1.3 Ma	900	1200	1500	3	3	3	ref[124]
Sanhe Cave	1.07-1.78 Ma	1070	1425	1780	4	4	4	ref[125]
Su Bang	Middle Pleistocene	129	451.5	774	1	2	2	ref[71]
Sunggu, Blora	163-248 ka	163	205.5	248	1	1	1	Rizal, n.d. cited in ref[71]
Tham Wiman Nakin	Middle Pleistocene (>160 ka)	160	467	774	1	2	2	ref[126]
Trinil	430-54o ka	430	485	540	2	2	2	ref[111]
Wajak	Late Pleistocene (>37.4 ka)	37.4	83.2	129	1	1	1	ref[127]

Data are from refs. [64,65,67,70–72,110,111,117–127].

Extended Data Table 6 | Stable isotope values for different orders of mammals across different geological subepochs and epochs of the Quaternary

Period		Mean $\delta^{13}C$	Mean $\delta^{18}O$	Stand. Dev $\delta^{13}C$	Stand. Dev $\delta^{18}O$
Early Pleistocene	Artiodactyla	-21.3	-5.9	7.3	1.9
	Carnivora	-24.2	-8.8	2.1	1.5
	Perissodactyla	-29.0	-8.6	0.7	2.3
	Primates	-24.3	-5.9	4.5	1.7
	Proboscidea	-18.1	-5.4	6.2	2.4
Middle Pleistocene	Artiodactyla	-16.4	-4.6	4.0	1.6
	Carnivora	-16.6	-5.6	4.7	0.9
	Perissodactyla	-24.4	-4.8	6.4	1.5
	Primates	-22.2	-5.4	4.3	1.3
	Proboscidea	-15.9	-6.0	3.8	1.2
	Rodentia	-21.9	-4.6	2.5	2.0
Late Pleistocene	Artiodactyla	-22.2	-6.2	5.8	1.4
	Carnivora	-20.0	-6.7	4.8	1.6
	Perissodactyla	-28.8	-6.3	3.8	1.3
	Primates	-24.7	-5.3	1.3	1.4
	Proboscidea	-29.4	-6.5	1.8	1.3
	Rodentia	-24.4	-5.8	0.7	0.5
Holocene	Artiodactyla	-23.5	-7.2	4.8	2.6
	Carnivora	-23.3	-7.3	3.8	1.8
	Perissodactyla	-29.1	-7.8	2.4	2.0
	Primates	-25.9	-6.6	2.1	2.2
	Proboscidea	-28.1	-6.4	2.3	0.9
	Rodentia	-23.8	-8.6	2.7	2.0